



## Specific surface area of a crushed welded tuff before and after aqueous dissolution

MICHAEL M. REDDY and HANS C. CLAASSEN

U.S. Geological Survey, Denver Federal Center, P.O. Box 25046, Denver, CO 80225, U.S.A.

(Received 4 August 1992; accepted in revised form 26 April 1993)

**Abstract**—Specific surface areas were measured for several reference minerals (anorthoclase, labradorite and augite), welded tuff and stream sediments from Snowshoe Mountain, near Creede, Colorado. Crushed and sieved tuff had an unexpectedly small variation in specific surface area over a range of size fractions. Replicate surface area measurements of the largest and smallest tuff particle size fractions examined (1–0.3 mm and <0.212 mm) were  $2.3 \pm 0.2 \text{ m}^2/\text{g}$  for each size fraction. Reference minerals prepared in the same way as the tuff had smaller specific surface areas than that of the tuff of the same size fraction. Higher than expected tuff specific surface areas appear to be due to porous matrix. Tuff, reacted in solutions with pH values from 2 to 6, had little change in specific surface area in comparison with unreacted tuff. Tuff, reacted with solutions having high acid concentrations (0.1 M hydrochloric acid or sulfuric-hydrofluoric acid), exhibited a marked increase in specific surface area compared to unreacted tuff.

### INTRODUCTION

ROCK AND mineral surface areas influence water quality by constraining reaction rates (LERMAN, 1979; DREVER and SWOBODA-COLBERG, 1989; HELGESON *et al.*, 1984; DAVIS and KENT, 1990; WHITE and PETERSON, 1990; CASEY *et al.*, 1989, 1991; CASEY and BUNKER, 1990; ANBEEK, 1992). While surface reactivity differs among rock and mineral types, laboratory studies demonstrate the importance of reactive surface area in mineral-water reactions. Rates of  $\text{CaCO}_3$  crystal growth, for example, are proportional to calcite surface area (REDDY and GAILLARD, 1981; REDDY *et al.*, 1981). Carbonate mineral crystallization and dissolution experiments use precipitated, high-purity seed crystals of uniform morphology and particle size (REDDY, 1983). Silicate dissolution experiments, on the other hand, employ crushed minerals, containing fractures, increased dislocation densities and surface damage. These mineral surface features may modify dissolution rates and confound interpretation of kinetic experiments (EGGLESTON *et al.*, 1989). Silicate mineral dissolution rate constants vary with mineral grain size; dissolution rates for fresh mineral surfaces are approximately two orders of magnitude higher than for naturally weathered surfaces (ANBEEK, 1992). In spite of intensive investigation, surface area influences on silicate mineral dissolution rates, and surface area modifications during dissolution are unclear (HELGESON *et al.*, 1984; WHITE and PETERSON, 1990; DAVIS and KENT, 1990; CASEY and BUNKER, 1990).

Rock and mineral surface characteristics are important in the interpretation of laboratory dissolution and field weathering experiments. Formation of a depleted or leached layer at the silicate mineral

reaction surface has been proposed by a number of investigators (HELGESON *et al.*, 1984; HELLMANN *et al.*, 1989; CASEY *et al.*, 1989, 1991; CASEY and BUNKER, 1990; SJOBERG, 1989; ALTHAUS and TIRTA-DINATA, 1989). A characteristic "parabolic" dissolution-rate law is consistent with a diffusion-rate-limiting step through such a leach layer (HOLDREN and ADAMS, 1982). This dissolution mechanism is not universally accepted for reactions at neutral pH, conditions which represent most natural weathering. Alternative dissolution mechanisms suggest that diffusion-limited kinetics result from the presence of secondary minerals formed on reacting surfaces during dissolution (DAVIS and KENT, 1990; WHITE and PETERSON, 1990). In contrast to kinetic theories assuming a diffusion process as the rate-limiting step, several investigators propose that silicate dissolution parabolic kinetics results from the presence of fine dust on mineral surfaces, and they propose treatment with hydrofluoric acid solution before silicate mineral dissolution experiments to eliminate "dust" artifacts (HOLDREN and BERNER, 1979; SCHÖTT *et al.*, 1981).

It is not clear which experimental procedures, such as mineral surfaces pretreatment, are appropriate to determine laboratory dissolution rate constants. Feldspar surfaces, for example, were altered during etching by HF (PERRY *et al.*, 1983). Acids preferentially leach reactive elements (such as  $\text{Na}^+$ ) and compounds (such as  $\text{CaCO}_3$ ) from mineral and rock surfaces, increase surface porosity, and cause grain disaggregation. Etchant-induced surface features may change rock or mineral surface areas, dissolution rates and reacting solution composition. ANBEEK (1992) has recently noted that the variety of mineral sample pretreatments confounds use of sur-

face area estimates in kinetic dissolution models.

This report describes the influence of rock pre-treatment and dissolution conditions on specific surface areas of a welded ash-flow tuff from the San Juan Mountains, in Colorado, specifically, Snowshoe Mountain quartz latite (RATTÉ and STEVEN, 1964). This task is part of a study of chemical weathering and reactive rock surface areas in watersheds on Snowshoe Mountain, Colorado (CLAASSEN *et al.*, 1983, 1986). An important application of the results of this study pertains to the use of welded tuff geological formations as repositories for long term nuclear waste storage.

We examined the distribution of minerals and matrix in the welded tuff among various particle size classes of crushed and sieved tuff. (Matrix, the petrographic term denoting the interstitial material lying between larger fragments, commonly used of igneous rock, is used here instead of the alternative term "groundmass" (ALLABY and ALLABY, 1991).) Tuff specific surface areas were measured before (fresh tuff surface) and after laboratory dissolution reactions (laboratory weathered tuff). Reference mineral (fresh surface) and several Snowshoe Mountain stream sediment (naturally weathered tuff) specific surface areas were also determined. Surface-area results presented here are limited to welded tuff from one location near the top of Snowshoe Mountain, sediment samples from three study watersheds on the north face of Snowshoe Mountain, and three reference minerals. Dissolution conditions included a range of solution acid concentrations and experimental configurations (REDDY and WERNER, 1987).

## EXPERIMENTAL METHODS

### Chemicals

Analytical reagent-grade chemicals, doubly-distilled deionized water, and Class A glassware were used throughout the study unless otherwise noted. Potassium bicarbonate solution (saturated with high purity CO<sub>2</sub> gas) or dilute HCl were background electrolytes for dissolution experiments.

### Tuff and minerals

Tuff samples used for surface area determination were obtained near the summit of Snowshoe Mountain, in the Seven Parks area (elevation 3350 m) (Snowshoe Mountain, 37°44'59"N 106°54'03"W, 3660 m, and Seven Parks (summit) 37°43'10"N 106°57'30"W, 3503 m) (CLAASSEN *et al.*, 1986). Colluvial rock samples were obtained from a 1.8 m hand-dug trench. A 10 kg rock (1.9 m from the surface, called TS-2) was crushed for mineralogical analyses, dissolution studies, pore size determinations and specific surface area measurements.

Tuff samples were crushed into small pieces by a steel jaw crusher and pulverised in a horizontal-shaft vertical-ceramic plate Braun pulveriser. Crushed rock intended for use in dissolution and specific surface-area studies was sieved into a number of size fractions, two of which are reported here:

Table 1. Sieve analysis of a Snowshoe Mountain tuff sample from the McKinney Gulch basin ground to pass 18 mesh

Size interval (mm)	Weight (%)	Cumulative weight (%)
>1.00	0.7	0.7
1.00-0.840	17.1	17.8
0.840-0.420	33.7	51.5
0.420-0.250	14.0	65.5
0.250-0.149	10.8	76.3
0.149-0.088	7.2	83.5
0.088-0.074	2.7	86.2
0.074-0.044	4.7	90.9
0.044-0.025	5.8	96.7
<0.025	3.3	100.0

<0.025, mud washed from rock during grinding and wet sieving.

(1) passing a 1.0 mm (18 mesh) sieve, but retained on a 0.3 mm sieve (50 mesh); and (2) passing a 0.212 mm sieve (70 mesh). The same crushing procedure and sieving sequence was also used for reference minerals examined. Several procedures (for example distilled water rinsing during sieving; dissolution in dilute HCl; dissolution in KHCO<sub>3</sub> solution saturated with CO<sub>2</sub> gas and etching with a H<sub>2</sub>SO<sub>4</sub>-HF) were used to remove fine particles on rock fragment surfaces prior to surface area measurements.

A reconnaissance tuff sample (from McKinney Gulch, elevation, 2680 m, on the NE face of Snowshoe Mountain), was crushed and sieved as described above to determine mineralogical abundance variations among tuff grain size classes. Particle-size weight-fraction distributions (Table 1) for this sample show that about half of the mass of the crushed rock possessed grain diameters between 1 mm and 0.42 mm.

Microscopic analysis of grain-mount thin sections of the crushed and sieved McKinney Gulch sample characterized the mineralogical composition (as volume percent) of each size fraction. Tuff grains from McKinney Gulch have varying matrix volume percents (from 59% to 42% for seven different size intervals, Table 2). The McKinney Gulch sample was enriched in matrix content in the coarse fraction, and depleted in matrix content in the fine fraction. Whole rock matrix contents for a sample from McKinney Gulch (Table 3, 47.3% matrix) and from the summit (Table 4, 43.1% matrix) have a matrix content in the range shown in Table 2. Snowshoe Mountain quartz latite has matrix content from 35% to 70% (RATTÉ and STEVEN, 1964).

Phenocrysts in the Seven Parks Summit whole-rock sample were mostly plagioclase (size, 0.2-1.8 mm) (An<sub>33</sub>), biotite (size, 0.4-1.4 mm), sanidine (size, 0.2-0.4 mm) and augite (size, 0.3-0.9 mm). This tuff composition can be compared with that of a naturally weathered and washed tuff-derived sediment sample (which passed through a 1.4 mm sieve) from the Deep Creek Basin on the north face of Snowshoe Mountain. The Deep Creek stream sediment was free of fine grain material and had an equal mixture of crystal fragments and rock fragments. The crystal fragments were mainly plagioclase (An<sub>30</sub>) with an estimated abundance in the crystal fraction of 75% (size, 0.06-1.25 mm). Augite and quartz were the next most abundant crystal fragments. Rock fragments in the Deep Creek sediment sample had approximately 70% matrix and 30% phenocrysts. The major crystal phase in the rock fragments is plagioclase (75%) (size, 0.05-0.9 mm). These sediment mineralogical analyses, which differ from the Seven Parks Summit analyses, suggest that the tuff has a mineral composition that varies with sample collection location and extent of weathering. The main point, however, is that matrix is a

Table 2. Tuff mineralogy for a sample from McKinney Gulch at the base of Snowshoe Mountain determined by microscopic thin-section examination of seven particle-size fractions

Phase	Particle-size fraction, volume %						
	>1.00	1.00-0.840	0.840-0.420	0.420-0.250	0.250-0.149	0.149-0.088	0.088-0.074
Matrix	55.7	55.5	55.9	59.4	47.4	44.9	42.0
Plagioclase	25.1	23.9	25.7	24.4	32.7	39.6	39.5
Augite	1.5	2.7	2.0	1.1	3.8	3.2	4.1
Biotite	7.1	6.8	6.5	7.2	7.1	4.5	5.1
Sanidine	1.1	2.1	2.2	2.6	3.3	3.2	3.0
Quartz	3.0	3.3	2.6	3.1	3.8	1.9	1.3
Opaque	2.6	3.3	1.8	1.6	0.8	1.4	2.4
Amphibole	1.1	—	—	0.6	0.4	—	—
Calcite	2.8	2.6	2.6	—	0.6	1.3	2.6
Zeolite	—	0.5	0.7	—	—	—	—

— phase not found in that mesh size interval.

Table 3. Tuff mineralogy for a whole rock sample from McKinney Gulch at the base of Snowshoe Mountain determined by microscopic thin section examination

Constituent	Volume (%)	Occurrence/texture/alteration
Quartz	3.2	Subhedral phenocrysts; 0.1-0.3 mm; partially embayed by matrix (resorbed).
Plagioclase	36.4	Subhedral phenocrysts; 0.4-2.1 mm; larger phenocrysts are zoned and somewhat fragmented; some are partially replaced by calcite; composition An <sub>33</sub> .
Sanidine	2.1	Subhedral phenocrysts; 0.2-0.5 mm; some phenocrysts are partially resorbed.
Augite	3.8	Subhedral phenocrysts; 0.2-0.7 mm; most are partially replaced by calcite along grain edges.
Biotite	4.5	Subhedral phenocrysts; 0.3-0.9 mm; most are relatively fresh; some altered along edges.
Opaque	1.8	Subhedral magnetite phenocrysts; 0.2-0.4 mm.
Hornblende	0.9	Subhedral phenocrysts; 0.2-0.5 mm; most grains are relatively fresh; some altered to opaques along edges.
Matrix	47.3	Microcrystalline; takes partial K-spar stain, probably composed mostly of sanidine and quartz; some replacement by calcite in vicinity of plagioclase or augite phenocrysts.

major component of Snowshoe Mountain welded tuff and the major tuff minerals (plagioclase, quartz, biotite, sanidine and augite) are found in all the rock and sediment samples.

"Reference mineral" samples (Ward Science Establishment,<sup>1</sup> Rochester, N.Y.) were used to identify sample preparation influences on surface areas of minerals similar to those of tuff phenocrysts (Table 4). Reference mineral

<sup>1</sup>The use of trade or firm names is for identification purposes only and does not constitute endorsement by the U.S. Geological Survey.

Table 4. Tuff mineralogy for a whole rock sample from Seven Parks summit area Snowshoe Mountain, Colorado determined by microscopic thin section examination.

Constituent	Volume (%)	Occurrence/texture/alteration
Quartz	2.1	Anhedral phenocrysts; 0.2-0.3 mm; embayed by matrix (resorbed).
Plagioclase	39.9	Subhedral to anhedral phenocrysts; 0.2-1.8 mm; composition An <sub>33</sub> .
Sanidine	3.2	Anhedral phenocrysts; 0.2-0.4 mm; partially resorbed by matrix.
Augite	2.5	Subhedral to anhedral phenocrysts; 0.3-0.9 mm; slightly leached along grain boundaries; some partially altered.
Biotite	6.3	Subhedral phenocrysts; 0.4-1.4 mm; most are relatively unaltered.
Opaque	2.0	Anhedral phenocrysts; 0.1-0.7 mm.
Hornblende	0.9	Anhedral phenocrysts; 0.2-0.5 mm.
Matrix	43.1	Microcrystalline; takes partial K-spar stain; some hair-like structures composed of hematite-limonite.

samples were: anorthoclase (light), Larvik, Norway; labradorite, Nain, Labrador, Canada; and pyroxene (augite), Harcourt Township, Ontario, Canada. Coarse (1-0.3 mm) and fine (<0.212 mm) size fractions were used for most surface area determinations reported here. Our hypothesis is that the phenocrysts in the tuff would have surface area changes during crushing that were similar to those of the reference minerals. Differences between the reference mineral and the tuff surface areas after crushing, we feel, could be attributed to the tuff matrix.

#### Dissolution experiments

Dissolution experimental conditions were planned to simulate selected features of weathering reactions at the base of the soil column in an alpine environment similar to

the summit of Snowshoe Mountain during a spring recharge event. In some experiments, low temperature (5°C) and high CO<sub>2</sub> partial pressures (about 0.8 atm) were used to minimize solution oxygen content (REDDY and WERNER, 1987). Experimental conditions minimized mechanical damage to reacting rock surfaces. Dissolution experiments lasted from less than 1 d to more than 1 a. Solid/solution mass ratios varied between 0.001 and 0.1.

The ionic strength and buffering capacity of solutions used in dissolution experiments were controlled by background electrolytes (HCl or KHCO<sub>3</sub> solution saturated with CO<sub>2</sub>). Potassium bicarbonate solutions were prepared by dissolving reagent-grade-KHCO<sub>3</sub> in distilled-deionized water. Before the start of each experiment, solution was transferred to the thermostatted reaction vessel. Solution pH, alkalinity and chemical composition of the starting solution, determined at the start of each experiment, agreed with values anticipated from the component solution compositions. Fisher Certified Concentrated HCl was diluted with distilled deionized water or with McKinney Gulch spring water for background electrolyte in experiments employing dilute HCl (REDDY and WERNER, 1987).

Iron concentrations in solution increased during tuff dissolution. Experimental conditions minimized the formation of hydrous iron oxides during tuff dissolution. For example, dissolution in KHCO<sub>3</sub> solution (pH 5–6) was done in a virtually oxygen-free environment (5°C, in 100% CO<sub>2</sub>).

#### Surface area measurements

Methods for determination of specific surface area have been recently summarized by DAVIS and KENT (1990). In this investigation, specific surface areas were measured in one of two ways: (1) a standard, multipoint, gravimetric BET gas adsorption procedure (ASTM Method No. 3663, Surface Area of Catalysts, done by Coors Spectro-Chemical Laboratory, Division of Coors Porcelain Company, Golden, Colorado); and (2) a method where the surface area is determined by adsorbing N from a flowing mixture of N and He (called here the dynamic BET method, ASTM Method No. D 3037 C surface area by continuous flow chromatography).

In the dynamic BET method, desorbed N gas is measured to determine the solid surface area using a Quantasorb instrument (manufactured by the Quantachrome Corp., Syosset, New York) (NELSEN and EGGERTSEN, 1958). Rock and mineral samples were outgassed at 200°C or 250°C for 30 min. Helium was the carrier gas (30% N<sub>2</sub>-70% He) for the region where N adsorption exhibits a linear BET adsorption isotherm. The cross sectional area of one adsorbed N<sub>2</sub> molecule (16.2 × 10<sup>-20</sup> m<sup>2</sup>) was used in the calculation of the surface area; tuff exhibited a linear BET isotherm plot up to reduced pressure values ( $P/P_0$ ) of 0.3. Subsequent to the work described here, surface areas were determined from time to time using other instruments. These values agree with the data obtained in this study.

Replicate specific surface area determinations for the same sample exhibit small deviations from the mean values (typically less than 5%, as relative percent deviation). Measurements of standard reference materials agreed within 10% of the known value. Surface area standards included an Al<sub>2</sub>O<sub>3</sub> (Quantachrome Cat. No. 2007, Lot No. 7008), which had a reported specific surface area of 1.97 m<sup>2</sup>/g. The standard Al<sub>2</sub>O<sub>3</sub>, when measured by the Quantachrome Corporation (outgas at 300°C for 30 min), was found to have a single point area (by N<sub>2</sub> at 0.3 relative pressure) of 1.92 m<sup>2</sup>/g, with a standard deviation based on six samples of 0.014 m<sup>2</sup>/g. We determined a mean specific surface area of 1.89 (± 0.064) m<sup>2</sup>/g for 14 determinations (outgas at 300°C for 30 min) over several weeks. The gravimetric BET procedure employed an NBS Mil-01 sur-

face area standard (with a known value of 10.7 ± 0.3 m<sup>2</sup>/g). This material gave values of 10.8 ± 0.6, 10.9, and 10.7 m<sup>2</sup>/g for three series of analyses.

#### Microscopy

Thin sections were prepared and examined by several commercial laboratories during the investigation. A Cambridge Scanning Electron Microscope was used for detailed examination of Au-coated tuff surfaces.

## RESULTS

### Surface area of unreacted reference minerals, Snowshoe Mountain tuff and watershed sediments

**Minerals.** Specific surface areas of crushed minerals (Table 5) varied as expected with grain size; surface area increased as particle size decreased (PARKS, 1990; WHITE and PETERSON, 1990). The small size fraction had specific surface areas of 0.31 to 1.26 m<sup>2</sup>/g. The coarse size fraction had specific surface areas that ranged from 0.06 to 0.30 m<sup>2</sup>/g. For comparison, the specific surface areas of the minerals can be expressed in units of m<sup>2</sup>/cm<sup>3</sup> by multiplying by the mineral density (anorthoclase, 2.6 g/cm<sup>3</sup>; augite 3.26 g/cm<sup>3</sup>; and labradorite, 2.7 g/cm<sup>3</sup>) (Table 5). Surface area differences among minerals in the same size fraction, expressed on a volume or weight basis, arise because of differences in mineral hardness and cleavage.

Volume normalized surface areas can be compared to calculated surface areas (expressed as area per volume of material) for cubes with fixed edge dimensions. This calculation shows that geometric surface areas (1 mm edge, 0.001 m<sup>2</sup>/cm<sup>3</sup> specific surface area; 0.1 mm edge, 0.01 m<sup>2</sup>/cm<sup>3</sup> specific surface area; and 0.001 mm edge, 1 m<sup>2</sup>/cm<sup>3</sup>) are one to two orders of magnitude smaller than measured volume normalized surface areas. Accessory minerals, surface fractures and dust on grain surfaces increase specific surface area above that expected for a fixed sieve size. The observation that crushed minerals commonly exhibit higher surface areas than that expected

Table 5. Particle-size range and specific surface areas (200°C outgas temperature, (30 min) using the dynamic method) for three crushed and sieved rock-forming reference minerals

Mineral	Particle-size range (mm)	Specific surface area	
		(m <sup>2</sup> /g)	(m <sup>2</sup> /cm <sup>3</sup> )
Labradorite	<0.212	0.96	2.6
Anorthoclase	<0.212	0.31	0.8
Pyroxene, augite	<0.212	1.26	4.1
Labradorite	1–0.3	0.30	0.8
Anorthoclase	1–0.3	0.06	0.2
Pyroxene, augite	1–0.3	0.06	0.2

Table 6. Crushed tuff particle-size range, BET method, outgas temperature, and specific surface areas

Particle-size range (mm)	BET method	Outgas temperature (°C)	Specific surface area (m <sup>2</sup> /g)
<0.212	Dynamic	200	2.73
1-0.3	Dynamic	200	2.09
1-0.3	Dynamic	275	2.26
<0.212	Gravimetric	300	2.26
1-0.3	Gravimetric	300	2.30

from their geometric grain size has been examined recently (PARKS, 1990; WHITE and PETERSON, 1990).

### Tuff

Specific surface areas of crushed and sieved tuff, measured by using either the gravimetric or the dynamic gas-adsorption method (Table 6), were greater than values of the corresponding size fractions of the reference minerals given in Table 5. Unlike the reference minerals, the surface area of the two tuff particle size fractions was nearly the same. Specific surface areas of the coarse- and fine-size fractions of the welded tuff are estimated to be 2.3 m<sup>2</sup>/g (with an estimated uncertainty of 0.2 m<sup>2</sup>/g).

Tuff (density 2.5 g/cm<sup>3</sup>) volume normalized surface area (5.8 m<sup>2</sup>/cm<sup>3</sup>) is an order of magnitude greater than that for the coarse fraction of the reference minerals and two orders of magnitude greater than the calculated geometric area. The Seven Parks tuff sample (Table 4) has about 50% matrix. Assuming phenocrysts contribute little to the surface area (as measurement of the reference minerals (Table 5) suggests), we estimate the matrix specific surface area to be about 4.6 ± 0.4 m<sup>2</sup>/g.

Outgas temperature (for the dynamic method) influenced tuff surface area values. Unpublished results for samples outgassed at room temperature (25°C) had good precision for replicate measurements (less than 5% relative deviation). However, specific surface areas for these samples were lower than samples outgassed at higher temperatures. The influence of outgas temperature on surface area measurements has been reported for labradorite following aqueous dissolution (CASEY *et al.*, 1989) and for microporous silica (GREGG and SING, 1982) and appears due to water desorption from the mineral surface (FU *et al.*, 1990).

### Snowshoe Mountain watershed sediments

Crushed tuff surface areas (Table 6), which are representative of fresh mineral surfaces, can be compared to naturally disaggregated and weathered, stream-water washed, tuff fragments in Snowshoe

Mountain watershed stream sediments. This comparison will identify differences between fresh and naturally-weathered tuff surfaces. Dried and sieved (<1.4 mm) sediment from streams near the base of Snowshoe Mountain had higher specific surface areas than expected for their respective particle sizes, or based on comparisons with reference minerals (Table 5) and unreacted tuff (Table 6). Specific surface areas (in m<sup>2</sup>/g) for 200°C outgas temperature were: McKinney Gulch, 8.9; Deep Creek, 4.4; and Gardiner Gulch, 5.6. Deep Creek stream sediment matrix content (approximately 35%) suggests a matrix area of 13 m<sup>2</sup>/g for naturally weathered tuff. This value, 4 times larger than that for fresh rock, may be due to the presence of hydrous metal oxides and clays in the stream sediments (WHITE, 1990; TARZL and PROTZ, 1978; BENSON and TEAGUE, 1982), or may be due to partial dissolution of the tuff matrix. The Snowshoe Mountain tuff-derived stream sediment surface areas are consistent with the observation that weathered rock fragments have higher surface areas than fragments formed by mechanical action (NIEMINEN *et al.*, 1985). As in the case of tuff surface area measurements, stream-sediment specific surface areas increased slightly with increasing outgas temperature.

### Aqueous dissolution influence on tuff surface area

Solutions of pH 2-6 caused little or no change in tuff specific surface area during dissolution. Tuff surface areas had small variation (1.4-2.6 m<sup>2</sup>/g, for 14 different experiments) for reacting solutions with a range of pH values (distilled water, KHCO<sub>3</sub> solutions saturated with CO<sub>2</sub>, and 0.01 M (initial concentration) HCl), solid to solution ratios and reaction times. Post-reaction surface areas for these reaction conditions are close to the estimated range of specific surface areas of the unreacted tuff (Table 6). Laboratory weathering by washing rock fragments with a variety of dilute acid solutions has little influence on tuff surface areas. This result suggests removal of fine particles from tuff surfaces has a small effect on surface area.

Tuff reacted in strongly acidic solutions (pH 1 or less) had significantly higher specific surface areas (Table 7) relative to unreacted tuff (Table 6) or tuff reacted in pH 2-6 solutions. Tuff dissolution in shaken polyethylene bottles with 0.1 M HCl (prepared with distilled water) had a specific surface area of 11.8 m<sup>2</sup>/g ± 0.5 m<sup>2</sup>/g (N = 4), a fivefold increase in tuff surface area during dissolution compared to unreacted tuff (Table 6) or tuff reacted with more dilute acid solutions. Tuff reacted with 0.1 M HCl prepared with McKinney Gulch spring water also increased in specific surface area (8.3 ± 0.3 m<sup>2</sup>/g) as did fine tuff (Table 7).

Increases in tuff surface area following dissolution in 0.1 N HCl can be compared with labradorite

Table 7. Tuff surface area following dissolution in (initially) 0.1 M HCl at 25°C. Solid-solution ratio, 0.1; particle-size range, 1–0.3 mm (unless otherwise noted); and reaction time of  $1.5 \times 10^4$  min in a shaken polyethylene bottle. Surface area was measured by using the dynamic method and a 200°C outgas temperature for 30 min.

Sample no.	Comment	Specific surface area (m <sup>2</sup> /g)
Acid diluted with distilled water		
1	0.04 g/g	6.1
3	—	10.9
9	—	12.0
11	—	12.0
13	—	12.4
15	<0.2 mm	12.7
Acid diluted with McKinney Gulch Spring water		
2	0.04 g/g	9.9
4	—	8.4
10	—	8.8
12	—	7.5
14	—	8.3
16	<0.2 mm	9.3

reacted 218 h in  $10^{-2}$  N HCl at 25°C, which had a final surface area of 6.2 m<sup>2</sup>/g (starting area 0.195 m<sup>2</sup>/g). This post-reaction labradorite surface area increase is attributed to spalling of a leached layer on the mineral surface (CASEY *et al.*, 1989).

Tuff surface areas also increased following etching of tuff grains. Etched tuff surface area was 5.3 m<sup>2</sup>/g. This surface area is smaller than that for tuff reacted with 0.1 M HCl, reflecting longer reaction times for samples treated with HCl. Etching solution, recommended for removal of dust from dissolving rocks and minerals, has a significant effect on the reacting surface of the tuff. Enstatite, reacted with H<sub>2</sub>SO<sub>4</sub>-HF etchant, is reported to have a higher surface area (0.55 m<sup>2</sup>/g) than similar size and treated diopside (0.06 m<sup>2</sup>/g) and tremolite (0.02 m<sup>2</sup>/g) (SCHOTT *et al.*, 1981).

Etched tuff reacted in a well-stirred batch reactor at 5°C in a  $10^{-2}$  M KHCO<sub>3</sub> solution saturated with CO<sub>2</sub> gas exhibited a slight decrease in specific surface area to 3.8 m<sup>2</sup>/g from a starting value of 5.3 m<sup>2</sup>/g (M. REDDY, unpublished data). In agreement with results of fresh tuff in solutions of pH 2–6, etch tuff dissolution in dilute KHCO<sub>3</sub>-H<sub>2</sub>CO<sub>3</sub> solution has little influence on reacting tuff surface area.

### Microscopy

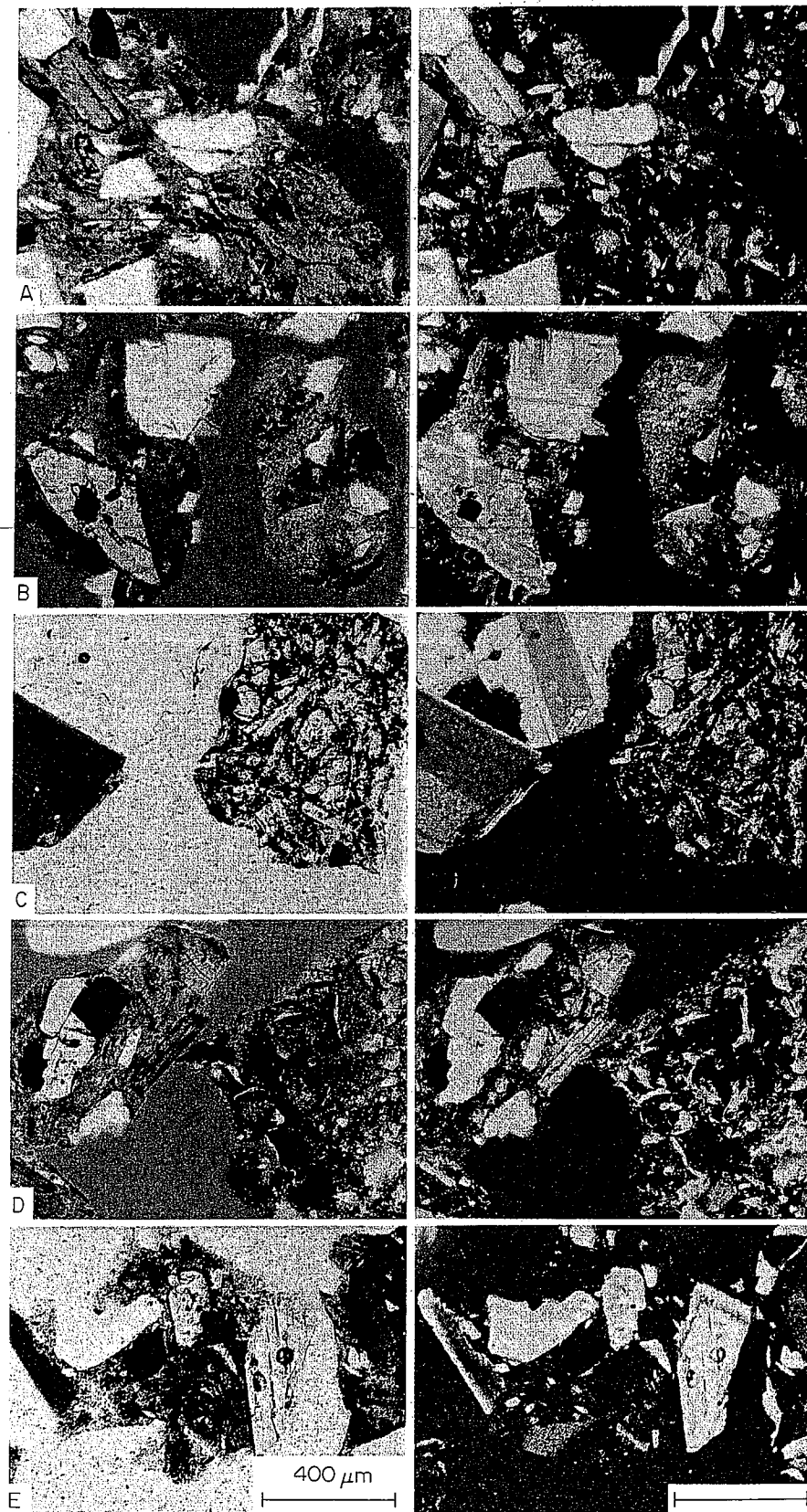
Fresh tuff was a light pink in hand specimens, with a lighter weathering rind on the surface of rocks. Thin section photomicroscopy (Fig. 1), with both bright-field illumination (at left in Fig. 1) and crossed polarizers (at right in Fig. 1), for unreacted tuff (Fig. 1A) illustrates phenocrysts (plagioclase and biotite) and matrix. Matrix banding apparent in micrographs is characteristic of a welded ash flow tuff. These laminae reflect a primary flow banding or bedding in the tuff. Several areas of blue dye impregnation are visible in the unreacted sample demonstrating extensive interconnected porosity in the grain.

The etched tuff sample (Fig. 1B) exhibits features seen in the unreacted sample, an augite phenocryst (on the left) and greater amounts of impregnated blue dye than the unreacted sample (most easily seen in the crossed polarized photomicrograph) consistent with its greater specific surface area. The Deep Creek stream sediment photomicrograph (Fig. 1C) has features absent in crushed tuff: (1) single mineral crystals free of matrix (biotite and plagioclase on the left); and (2) porous particle aggregates (on the right of Fig. 1C). Individual crystal fragments indicate tuff matrix is removed from phenocrysts in the stream. Accumulation of porous aggregates, perhaps cemented by hydrous metal oxides, may contribute to the high specific surface area exhibited by the stream sediments.

Tuff grains dissolved in bicarbonate solution (Fig. 1D; with blue stained epoxy) also contained porous aggregates, shown by the areas impregnated by blue dye (Fig. 1D). Tuff dissolved in the most acidic solutions (Fig. 1E) shows similarities to the other micrographs; however, the grain boundaries appear to have undergone matrix dissolution. In particular, it appears that the matrix was dissolved from the surface of the augite phenocrysts in the center of the photomicrograph. Augite phenocrysts appear to have etch features as well.

Tuff surface features not apparent in optical microscopy can be observed with scanning electron microscopy (Fig. 2). Tuff fragments sonicated for 108 min in distilled water exhibit both smooth surface features of phenocrysts and a mottled texture of matrix. A porous matrix surface and fractures are apparent on the surface of the unreacted grain (Fig. 2A) and the etched grain (Fig. 2B). Tuff reacted in 0.01 M HCl (Fig. 2C) has slightly greater surface texture and apparent porosity than the unreacted tuff. Etch pits

Fig. 1. (Opposite). Optical micrographs of Snowshoe Mountain tuff grains (brightfield illumination on the left, crossed polarizers on the right, marker = 400 μm): A. Unreacted grains embedded in blue epoxy. Blue color in the interior of grains shows areas of internal porosity (surface area = 2.3 m<sup>2</sup>/g); B. Grains etched with H<sub>2</sub>SO<sub>4</sub>-HF for 6 min (surface area = 5.3 m<sup>2</sup>/g); C. Stream sediment grains from Deep Creek near the base of Snowshoe Mountain (surface area = 4.4 m<sup>2</sup>/g); D. Grains reacted in 0.01 M KHCO<sub>3</sub> solution at 5°C with 100% CO<sub>2</sub> gas for 578,000 min (surface area = 2.2 m<sup>2</sup>/g); E. Grains dissolved in 0.1 M HCl for 18,300 min (surface area = 11.8 m<sup>2</sup>/g).



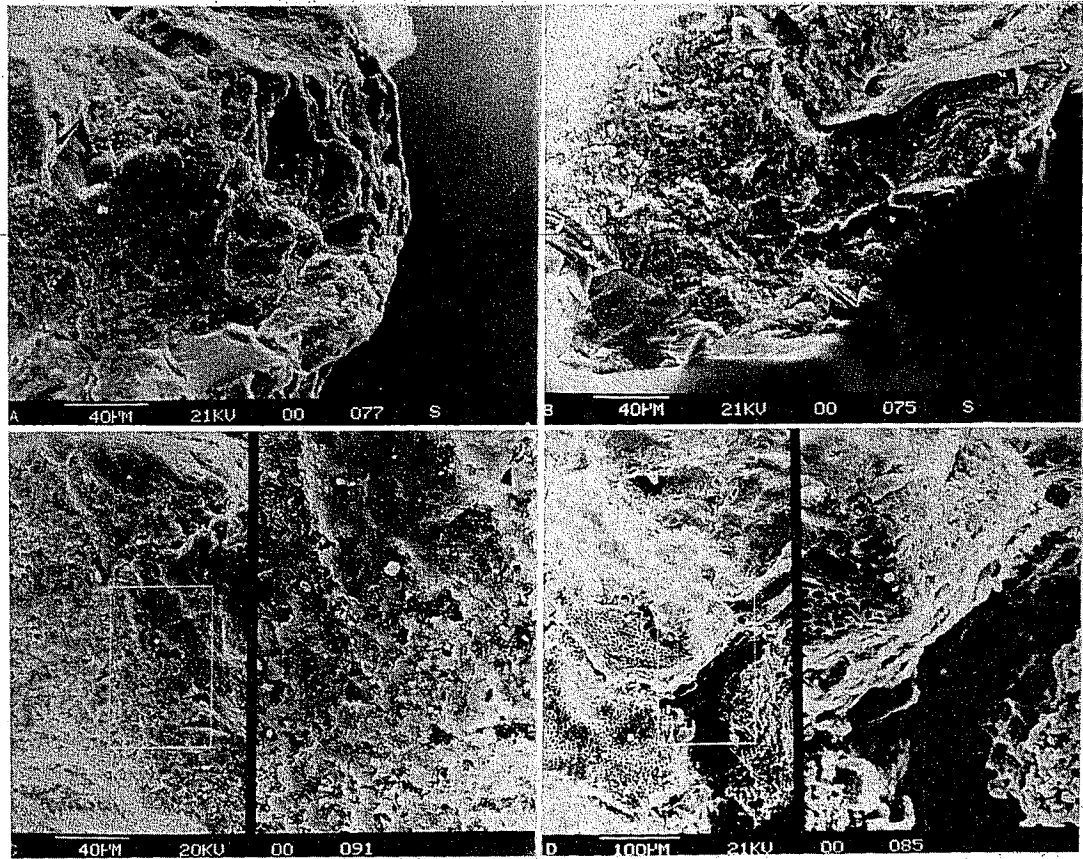


FIG. 2. Scanning electron micrographs of Snowshoe Mountain tuff grains: A. Grains sonicated with distilled water for 108 min (surface area =  $2.7 \text{ m}^2/\text{g}$ ); B. Grains etched with  $\text{H}_2\text{SO}_4\text{-HF}$  for 6 min (surface area =  $5.3 \text{ m}^2/\text{g}$ ); C. Grains dissolved in 0.01 M HCl for 12,910 min (surface area =  $2.2 \text{ m}^2/\text{g}$ ); D. Grains dissolved in 0.1 M HCl for 18,300 min (surface area =  $11.8 \text{ m}^2/\text{g}$ ).

and particulates are visible on this grain surface. Tuff reacted in 0.1 M HCl (Fig. 2D) showed marked surface alteration. Etch pits on grain surfaces and a porous aggregate particles are consistent with the higher surface area of the tuff reacted in 0.1 M HCl compared to fresh tuff.

### DISCUSSION

Tuff surface areas and surface area changes following strong acid pretreatment or dissolution exhibit three notable aspects. First, unreacted tuff and tuff-derived stream sediments from Snowshoe Mountain watersheds have surface areas greater than anticipated from particle size and from comparison with three reference minerals prepared in the same way as the tuff. Second, tuff surface area increased over that of the fresh mineral surface following dissolution in strongly acid solutions. Third, tuff-derived stream sediments have higher surface areas than freshly crushed rock and laboratory weathered tuff.

Hypotheses consistent with the larger than expected specific surface area of the unreacted tuff and the stream sediments include: (1) the tuff matrix has extensive intergranular porosity, perhaps associated with a small matrix particle size; (2) tuff and stream sediments contain a high surface-area dust; and (3) tuff and stream sediments contain hydrous metal oxides or clays. These hypotheses will be briefly examined.

The presence of a porous, high specific surface area tuff matrix appears to be the source of the surface properties observed for Snowshoe Mountain tuff. Porous pumice blocks have been reported for Snowshoe Mountain quartz latite (RATTÉ and STEVEN, 1967). Snowshoe Mountain tuff porosity ranges from 2 to 10% (RATTÉ and STEVEN, 1964). Tuff cut for experiments reported in this paper has internal voids (diameter from 0.1 to 1 mm) and macroscopic porosity. This porosity is also apparent in blue epoxy impregnated tuff thin sections (Fig. 1A).

Snowshoe Mountain tuff slabs several mm on an edge were examined to test the hypothesis that tuff matrix is porous and has a high specific surface area. Mercury intrusion porosimetry of these slabs, a measure of larger pore diameters, gave values of: 4.7% porosity and 0.0178  $\mu\text{m}$ , mean pore diameter. Nitrogen adsorption/desorption, a measure of small pores gave values of: 1.3% porosity; 0.95  $\text{m}^2/\text{g}$ , surface area and 0.0187  $\mu\text{m}$ , average pore diameter. These results support the hypothesis that the Snowshoe Mountain tuff matrix is a porous, high surface area material. We thus conclude that high specific surface area of the Snowshoe Mountain tuff is associated with extensive microporosity in the microcrystalline sanidine and quartz matrix (CLAASSEN *et al.*, 1983). A summary of the experimental procedures and corresponding surface areas is shown below.

Examination of tuffs from other locations may give insight into processes which lead to formation of a high surface area matrix. Bishop Rhyolitic tuff, for example, has inclusions which may cause increased surface area. These inclusions were formed in gas-saturated decompressing magma during phenocryst growth (ANDERSON, 1991). In addition, other processes such as cooling quartz crystals, which undergo 1% volume contraction (GHIORSO *et al.*, 1979), will lead to an increase in matrix porosity. Snowshoe Mountain tuff matrix porosity appears to result from its depositional history.

Dust on the surfaces of the tuff coarse-size fraction appears to contribute little to the measured specific surface area. Tuff reacted in acid solutions and tuff stream sediments are free of attached fine particles (Fig. 2). Scanning electron microscopy and microscopy demonstrate that both distilled water washing and dissolution treatments remove dust from grain surfaces. Neither water washing nor extensive dissolution at pH 5–6 decreased tuff specific surface area. If dust on tuff grain contributed to the measured surface area, dust removal by washing or dissolution would lower surface area values.

Etching with  $\text{H}_2\text{SO}_4$ -HF solution also removes

Tuff surface area summary  
TUFF (cubes several mm on edge—1  $\text{m}^2/\text{g}$ )

Tuff-derived stream sediments (<1.4 mm, 4–9 $\text{m}^2/\text{g}$ ) (Naturally weathered)	Tuff crushed and sieved (1–0.3 mm and <0.212 mm, 2.3 $\text{m}^2/\text{g}$ (Fresh surface)	HF- $\text{H}_2\text{SO}_4$ Tuff pretreatment (1–0.3 mm, 5.3 $\text{m}^2/\text{g}$ )
KHCO <sub>3</sub> -H <sub>2</sub> CO <sub>3</sub> , or 0.01 N HCl dissolution, 5 or 25°C (1–0.3 mm, 1.4 to 2.6 $\text{m}^2/\text{g}$ )	0.1 N dissolution, 25°C (1–0.3 mm, <0.212 mm, 6 to 12 $\text{m}^2/\text{g}$ )	Tuff dissolution (Laboratory weathered) KHCO <sub>3</sub> -H <sub>2</sub> CO <sub>3</sub> Dissolution, 5°C (1–0.3 mm, 3.8 $\text{m}^2/\text{g}$ )

dust from mineral surfaces (Fig. 2B). However, this procedure increases tuff specific surface area. A surface area increase due to etching is the opposite of that anticipated if surface dust caused high specific surface area values. Surface area of each of these tuff-treatments is the same or greater than fresh tuff, even though surface dust was removed by these treatments. Tuff surface area increases following weathering or dissolution in strong acid solutions may result from both modification of the matrix and formation of secondary minerals (WHITE, 1990; TARZI and PRÖTZ, 1978; BENSON and TEAGUE, 1982).

### CONCLUSIONS

High specific surface areas for Snowshoe Mountain tuff reflect the presence of a porous matrix. Tuff specific surface areas change little during extended aqueous dissolution in solutions of initial pH 2–6. Acid etch treatment and strong acid (0.1 M HCl) dissolution caused a significant increase in post-reaction tuff surface area. Results obtained here suggest that tuff pretreatment prior to dissolution kinetics experiments should not include strong acid washes or H<sub>2</sub>SO<sub>4</sub>-HF etchants to remove fine particulate material. Treatment with dilute HCl and CO<sub>2</sub> saturated KHCO<sub>3</sub> solutions (pH 2–6) does not appear markedly to alter the tuff surface area, even after extended periods of reaction, and would thus be appropriate for tuff pretreatment prior to dissolution experiments.

*Acknowledgements*—The authors wish to acknowledge the assistance of M. Werner, R. Cygan and M. Nienow in collecting rock samples from Snowshoe Mountain. M. Werner conducted dissolution experiments and sample analysis. T. Thompson and M. Werner carried out dynamic gas adsorption surface area measurements. Mineralogical analyses of thin sections were done by either R. Kurvill or F. Fisher, both of Denver, CO.

*Editorial handling*: Y. Kharaka.

### REFERENCES

- ALLABY A. and ALLABY M. (1991) *The Concise Oxford Dictionary of Earth Sciences*. Oxford University Press.
- ALTHAUS E. and TIRTADINATA E. (1989) Dissolution of feldspar: The first step. In *Water-Rock Interaction* (ed. D. L. MILES), pp. 15–17. Proc. 6th Intern. Symp. Water-Rock Interaction, Malvern, Balkema, Rotterdam.
- ANBEEK C. (1992) The dependence of dissolution rates on grain size for some fresh and weathered feldspars. *Geochim. cosmochim. Acta* **56**, 3957–3970.
- ANDERSON A. T., JR. (1991) Hourglass inclusions: Theory and application to the Bishop Rhyolitic Tuff. *Am. Miner.* **76**, 530–547.
- BENSON L. V. and TEAGUE L. S. (1982) Diagenesis of basalts from the Pasco Basin, Washington I. Distribution and composition of secondary mineral phases. *J. Sed. Pet.* **52**, No. 2, 595–613.
- CASEY W. H. and BUNKER B. (1990) Leaching of mineral and glass surfaces during dissolution. In *Reviews of Mineralogy Volume 23 Mineral-Water Interface Geochemistry* (eds M. F. HOCELLA, JR. and A. F. WHITE), pp. 397–426. *Mineral. Soc. of Amer.*, Washington, D.C.
- CASEY W. H., WESTRICH H. R. and HOLDREN G. R. (1991) Dissolution rates of plagioclase at pH = 2 and 3. *Am. Miner.* **76**, 211–217.
- CASEY W. H., WESTRICH H. R., MASSIS T., BANFIELD J. F. and ARNOLD G. W. (1989) The surface of labradorite feldspar after acid hydrolysis. *Chem. Geol.* **78**, 205–218.
- CLAASSEN H. C., REDDY M. M. and HALM D. R. (1986) Use of the chloride ion in determining hydrologic-basin budgets—A 3-year case study in the San Juan Mountains, Colorado, U.S.A. *J. Hydrol.* **85**, 49–71.
- CLAASSEN H. C., REDDY M. M. and WHITE A. F. (1983) Relationship between precipitation and vadose-zone chemistry in a high-altitude watershed in Colorado. In *Proceedings of the Fifth Annual Participants' Information Meeting, DOE Low-Level Waste Management Program, August 30–September 1, 1983* (ed. E. G. IDAHO & G, Inc.), pp. 726–736. U.S. Department of Energy under DOE Contract No. AC07-76ido1570, Idaho Falls, Idaho.
- DAVIS J. A. and KENT D. B. (1990) Surface complexation modeling in aqueous geochemistry. In *Reviews in Mineralogy Volume 23 Mineral-water Interface Geochemistry* (eds M. F. HOCELLA, JR. and A. F. WHITE), pp. 177–260. *Mineral. Soc. Amer.*, Washington, D.C.
- DREVER I. J. and SWOBODA-COLBERG N. (1989) Mineral weathering rates in acid-sensitive catchments: Extrapolation of laboratory experiments to the field. In *Water-Rock Interaction* (ed. D. L. MILES), pp. 211–214. Proc. 6th Intern. Symp. Water-Rock Interaction, Malvern, Balkema, Rotterdam.
- EGGLESTON C. M., HOCELLA M. F. and PARKS G. A. (1989) Sample preparation and aging effects on the dissolution rate and surface composition of diopside. *Geochim. cosmochim. Acta* **53**, 797–804.
- FU M. H., ZHANG Z. Z. and LOW P. F. (1990) Changes in the properties of a montmorillonite-water system during the adsorption and desorption of water; Hysteresis. *Clays Clay Miner.* **38**, No. 5, 485–492.
- GHIORSO M. S., CARMICHAEL I. S. E. and MORET L. K. (1979) Inverted high-temperature quartz; unit cell parameters and properties of the alpha-beta inversion. *Mineral. and Petrol.* **68**, 307–323.
- GREGG S. J. and SING K. S. (1982) *Adsorption, Surface Area and Porosity*. Academic Press.
- HELGESON H. C., MURPHY W. M. and AAGAARD P. (1984) Thermodynamic and kinetic constraints on reaction rates among minerals and aqueous solutions. II: Rate constants, effective surface areas, and the hydrolysis of feldspar. *Geochim. cosmochim. Acta* **48**, 2405–2432.
- HELLMANN R., EGGLESTON C. M., HOCELLA M. F., JR. and CRERAR D. A. (1989) Altered layers on dissolving albite. Part 1. Results. In *Water-Rock Interaction* (ed. D. L. MILES), pp. 218–296. Proc. 6th Intern. Symp. Water-Rock Interaction, Malvern, Balkema, Rotterdam.
- HOLDREN G. R., JR. and ADAMS J. E. (1982) Parabolic dissolution kinetics of silicate minerals: An artifact of nonequilibrium precipitation process? *Geol.* **10**, No. 4, 186–190.
- HOLDREN G. R., JR. and BERNER R. A. (1979) Mechanism of feldspar weathering, Part I. Experimental studies. *Geochim. cosmochim. Acta* **43**, 1161–1171.
- LERMAN A. (1979) *Geochemical Processes Water and Sediment Environments*. John Wiley & Son, Inc.
- NELSEN F. M. and EGGERTSEN F. T. (1958) Determination of surface area adsorption measurements by a continuous flow method. *Analyt. Chem.* **30**, 1387–1390.
- NIEMINEN P., SALOMAA R. and UUSINOKA R. (1985) The use of specific surface area, pore volume, and pore area in evaluating the degree of weathering of fine particles: An example from Lauhanvuori, western Finland. *Fennia* **163**:2, 373–377.

- PARKS G. A. (1990) Surface energy and adsorption at mineral-water interfaces: An introduction. In *Reviews in Mineralogy Volume 23 Mineral-water Interface Geochemistry* (eds M. F. HOCELLA, JR. and A. F. WHITE), pp. 133-175. *Mineral. Soc. Amer., Washington, D.C.*
- PERRY D. L., TSAO L. and GAUGLER K. A. (1983) Surface study of HF and HF/H<sub>2</sub>SO<sub>4</sub>-treated feldspar using auger electron spectroscopy. *Geochim. cosmochim. Acta* **47**, 1289-1291.
- RATÉ J. C. and STEVEN T. A. (1964) Magmatic differentiation in a volcanic sequence related to the Creede Caldera, Colorado. *U.S. Geol. Surv. Prof. Paper* **475-D**, D49-D53.
- RATÉ J. C. and STEVEN T. A. (1967) Ash flows and related volcanic rocks associated with the Creede Caldera San Juan Mountains, Colorado. *U.S. Geol. Surv. Prof. Paper* **524-H**, H1-H58.
- REDDY M. M. (1983) Characterization of calcite dissolution and precipitation using an improved experimental technique. *Sci. Geol. Mem.* **71**, 109-117.
- REDDY M. M. and GAILLARD W. D. (1981) Kinetics of calcium carbonate (calcite)-seeded crystallization: The influences of solid-solution ratio on the reaction constant. *J. Coll. Inter. Sci.* **80**, No. 1, 171-178.
- REDDY M. M., PLUMMER L. N. and BUSENBERG E. (1981) Crystal growth of calcite from calcium bicarbonate solutions at constant carbon dioxide partial pressures and 25°C: A test of a calcite dissolution model. *Geochim. cosmochim. Acta* **45**, No. 8, 1281-1289.
- REDDY M. M. and WERNER M. G. (1987) Data from laboratory dissolution experiments using a welded tuff from Snowshoe Mountain near Creede, Colorado. *U.S. Geol. Surv. Open-File Report* **87-550** **87**, 1-23.
- SCHOTT J., BERNER R. A. and SJOBERG E. L. (1981) Mechanism of pyroxene and amphibole weathering, I. experimental studies of iron-free minerals. *Geochim. cosmochim. Acta* **45**, 2123-2135.
- SJOBERG E. L. (1989) Kinetics and non-stoichiometry of labradorite dissolution. In *Water-Rock Interaction* (ed. D. L. MILES), pp. 639-642. Proc. 6th Intern. Symp. Water-Rock Interaction, Malvern, Balkema, Rotterdam.
- TARZL J. G. and PRÖTZ R. (1978) Characterization of morphological features of soil micas using scanning electron microscopy. *Clays Clay Miner.* **26**, 352-360.
- WHITE A. F. (1990) Heterogeneous electrochemical reactions associated with oxidation of ferrous oxide and silicate surfaces. In *Review in Mineralogy Volume 23 Mineral-water interface geochemistry* (eds M. F. HOCELLA, JR. and A. F. WHITE), pp. 467-509. *Mineral. Soc. Amer., Washington, D.C.*
- WHITE A. F. and PETERSON M. L. (1990) Role of reactive-surface-area characterization in geochemical kinetic models. In *Chemical modeling of aqueous systems II* (eds D. C. MELCHIOR and R. L. BASSETT), pp. 461-475. *Amer. Chem. Soc. Washington, D.C.*